Weather and Climate Extremes 51 (2026) 100861

Contents lists available at ScienceDirect

Weather and Climate Extremes

journal homepage: www.elsevier.com/locate/wace

Has the fire weather index emerged? Insights from global and regional climate models

Rita Nogherotto [a,b,*], Francesca Raffaele [b,c], Graziano Giuliani [c], Erika Coppola [c]

[a] Institute of Atmospheric Sciences and Climate (CNR-ISAC), Italy
[b] National Institute of Oceanography and Applied Geophysics (OGS), Italy
[c] The Abdus Salam International Centre for Theoretical Physics (ICTP), Italy

A B S T R A C T

Wildfires are expected to become more intense due to global warming. This change will significantly affect ecosystems and communities. We examine when and where fire weather conditions go beyond natural variability by using the Canadian Fire Weather Index (FWI). We analyze data from CORDEX-CORE and EURO-CORDEX regional simulations, along with CMIP5 and CMIP6 global models, under the RCP8.5 and SSP5-8.5 scenarios. The study spans from 1980 to 2099 and focuses on Global Warming Levels (GWLs) ranging from +1.5 to +4.0 °C compared to pre-industrial climate.

When we evaluate against GEFF-ERA5 reanalysis, we find that the CORDEX ensemble better reflects historical FWI trends compared to CMIP5 and CMIP6. Projections show widespread increases in FWI, primarily due to higher temperatures and lower relative humidity, along with regional impacts from precipitation and wind. The danger class analyses indicate a shift toward Extreme and Very Extreme conditions in the Mediterranean, southern Africa, South America, and Australia, occurring already with 2–3 °C of warming.

The Time of Emergence (ToE) analysis reveals that human influence is already detectable in 39% of the AR6 regions, to become 81% by 2030. The Global Temperature of Emergence (GToE) suggests that over 25% of burnable land areas will cross emergence thresholds at +1.5 °C, increasing to over 70% at +3.0 °C. The length of the fire season is also expected to increase in most regions. These findings highlight the urgent need for strategies to manage wildfire risk and adapt to these changes globally.

Key points

- Regional climate models (CORDEX) more accurately reproduce historical fire-weather conditions compared to CMIP5/CMIP6 global models.
- Widespread increases in extreme fire-weather conditions emerge under 2–3 °C of global warming, especially in the Mediterranean, southern Africa, Amazonia, Central America and Southern Australia.
- Human influence on fire weather is already detectable in ~40% of AR6 regions, increasing to >80% by 2030.
- Fire season length is projected to increase in most fire-prone regions, amplifying risks to ecosystems and communities.
- Results provide geographically- and temporally-specific guidance for wildfire adaptation planning.

1. Introduction

Wildfires represent a growing and severe threat to ecosystems, communities, and economies worldwide. Understanding drivers of fire activity is crucial for developing effective strategies in wildfire management, mitigation, and adaptation in a changing climate. Over the past half century, global fire activity has been documented to increase in several parts of the world (Kasischke and Turetsky, 2006; Westerling, 2016).

This upward trend in wildfires is attributed to a complex interplay of factors, including climate change, land-use changes, and human activities. Weather and climate play a crucial role in determining the fire regime of an area (Viegas and Viegas, 1994; Pyne, 1996; Skinner et al., 1999; Kunkel, 2001; Viegas et al., 2001; Pereira et al., 2005). Therefore, shift in climatic conditions can significantly enhance wildfire activity in many areas.

To better understand the meteorological drivers that determine a persistent fire activity once ignition has occurred, the scientific community has been extensively studying fire behavior. It is intuitive that dry, live fuels tend to ignite more easily than moist fuel when low

* Corresponding author. Institute of Atmospheric Sciences and Climate (CNR-ISAC, Italy), Italy
E-mail address: r.nogherotto@isac.cnr.it (R. Nogherotto).

https://doi.org/10.1016/j.wace.2026.100861
Received 22 October 2025; Received in revised form 4 December 2025; Accepted 23 January 2026
Available online 28 January 2026

Table 1
CORDEX-CORE and EURO-CORDEX RCMs and their corresponding driving GCM used in this study.

Driving GCM	Ensemble	CORDEX-CORE 0.22	CORDEX region
CNRM-CM5	r1i1p1	GERICS-REMO2015	EUR
CNRM-CM5	r1i1p1	SMHI-RCA4	EUR
EC-EARTH	r1i1p1	DMI-HIRHAM5	EUR
EC-EARTH	r1i1p1	KNMI-RACMO22E	EUR
EC-EARTH	r1i1p1	SMHI-RCA4	EUR
EC-EARTH	r12i1p1	CLMcom-ETH-COSMO-crCLIM-v1-1	EUR
EC-EARTH	r12i1p1	DMI-HIRHAM5	EUR
EC-EARTH	r12i1p1	KNMI-RACMO22E	EUR
EC-EARTH	r12i1p1	MOHC-HadREM3-GA7-05	EUR
EC-EARTH	r12i1p1	SMHI-RCA4	EUR
EC-EARTH	r3i1p1	KNMI-RACMO22E	EUR
EC-EARTH	r3i1p1	SMHI-RCA4	EUR
GFDL-ESM2M	r1i1p1	ICTP-RegCM4-7	CAM, NAM
HadGEM2-ES	r1i1p1	CNRM-ALADIN63	EUR
HadGEM2-ES	r1i1p1	ICTP-RegCM4-6	EUR, AUS, AFR, CAM, EAS, SAM, SEA, NAM
HadGEM2-ES	r1i1p1	KNMI-RACMO22E	EUR
HadGEM2-ES	r1i1p1	MOHC-HadREM3-GA7-05	EUR
HadGEM2-ES	r1i1p1	GERICS-REMO2015	AUS, AFR, CAM, EAS, NAM, SAM, SEA, WAS
IPSL-CM5A-MR	r1i1p1	GERICS-REMO2015	EUR
IPSL-CM5A-MR	r1i1p1	KNMI-RACMO22E	EUR
MIROC5	r1i1p1	ICTP-RegCM4-6	WAS
MPI-ESM-LR	r1i1p1	CLMcom-ETH-COSMO-crCLIM-v1-1	EUR
MPI-ESM-LR	r1i1p1	CNRM-ALADIN63	EUR
MPI-ESM-LR	r1i1p1	DMI-HIRHAM5	EUR
MPI-ESM-LR	r1i1p1	ICTP-RegCM4-6	EUR, NAM
MPI-ESM-LR	r1i1p1	KNMI-RACMO22E	EUR
MPI-ESM-LR	r1i1p1	SMHI-RCA4	EUR
MPI-ESM-LR	r1i1p1	GERICS-REMO2015	AFR, AUS, CAM, EAS, EUR, NAM, SAM, SEA, WAS
MPI-ESM-LR	r2i1p1	CLMcom-ETH-COSMO-crCLIM-v1-1	EUR
MPI-ESM-LR	r2i1p1	SMHI-RCA4	EUR
MPI-ESM-LR	r3i1p1	GERICS-REMO2015	EUR
MPI-ESM-LR	r3i1p1	SMHI-RCA4	EUR
MPI-ESM-MR	r1i1p1	ICTP-RegCM4-6	AFR, AUS, CAM, EAS, SAM, SEA, WAS
NorESM1-M	r1i1p1	CLMcom-ETH-COSMO-crCLIM-v1-1	EUR
NorESM1-M	r1i1p1	GERICS-REMO2015	EUR, AUS, AFR,CAM, EAS, NAM, SAM, SEA, WAS
NorESM1-M	r1i1p1	KNMI-RACMO22E	EUR
NorESM1-M	r1i1p1	SMHI-RCA4	EUR
NorESM1-M	r1i1p1	ICTP-RegCM4-6	EUR, AUS, AFR, EAS, SAM, SEA, WAS

Table 2
CMIP5 Models used in this study.

CMIP5	Ensemble
NorESM1-M	r1i1p1
MPI-ESM-MR	r1i1p1
MPI-ESM-LR	r1i1p1
HadGEM2-ES	r1i1p1

humidity and high temperature are combined. Additionally, compared to situations when wind primarily blows in one prevailing direction, considerable wind variability supports the spread over broader areas. As a result of climate change, fire weather and the likelihood of fire events are expected to rise in many regions around the world, including areas that have historically been less prone to wildfires (Masson-Delmotte et al.). Meteorologically, the risk of fire ignition rises with higher temperatures, stronger winds, and lower relative humidity. Projected changes in these variables are expected to more than double the frequency of extreme fire weather events by the end of the 21st century (Touma et al., 2021), while also increasing the duration, severity, and geographic reach of fires (Bowman et al., 2020; Fargeon et al., 2020; Ruffault et al., 2020; De Rigo et al., 2017).

It is possible to study projections of fire risk under climate change by means of fire indices, such as the Canadian Forest Fire Weather Index (FWI; van Wagner, 1987), the U.S. Forest Service's National Fire Danger Rating System (NFDRS; Larry S. et al., 1984), or Australia's McArthur Rating System (Mark 5; McArthur, 1967). These indices are statistical models that capture the relationship between fire occurrences and weather conditions. They have been shown to provide reliable assessments of fire danger in both short- and long-term weather forecasts worldwide (Di Giuseppe et al., 2016).

In this study we use the FWI from the Canadian Forest Fire Weather Index System, one of the most extensively used models to estimate fire danger globally (as noted in Di Giuseppe et al., 2016; Field, 2020; de Groot et al., 2013). The FWI is particularly suitable in this context because it represents potential fire intensity associated with fuel dryness and fire weather conditions, and is independent of land cover and biomass type. It is highly sensitive to changes in temperature, precipitation, humidity, and wind speed (Flannigant et al., 2016) and shows strong empirical associations with burned areas across extensive regions of the world (Abatzoglou et al., 2018).

Earlier research (e.g., Flannigan et al., 2013) has examined changes in global fire weather metrics under anthropogenic climate change using global climate models (Bedia and Bhend, 2015; Williams and Abatzoglou, 2016). However only a few studies have explicitly deterined when or whether observed changes can be attributed to anthropogenic influences rather than internal climate variability (Abatzoglou et al., 2016).

In this study, we instead analyze the full set of high-resolution regional climate CORDEX-CORE simulations, enabling a more region-specific assessment of climate-driven shifts in fire weather. Regional climate models better represent local-scale processes and feedbacks that strongly influence changes in precipitation, humidity and wind patterns, key drivers of fire danger.

We evaluate the results within the time of emergence (ToE) framework. The ToE concept is central to understand when the anthropogenic climate-change signal becomes statistically distringuishable from the background natural climate variability. It therefore provides insight into the timeframe over which human-driven changes in fire-weather conditions become unavoidable and relevant for adaptation planning.

2. Data and methods

2.1. CORDEX-CORE climate projections

In this analysis, we use simulations from 31 CORDEX-CORE simulations (Table 1) at 0.22° resolution over the NAM, SAM, CAM, AFR, AUS, WAS, EAS and SEA domains, and at 0.11° resolution over the EURO-CORDEX domain. The second ensemble used for comparison consists of the driving global simulations used for the CORDEX-CORE experiments (Table 2), from the Fifth Phase of the Coupled Model Intercomparison Project CMIP5 (Taylor et al., 2012). As a third ensemble, we analyze 7 simulations from CMIP6 (Eyring et al., 2016) (Table 3). The choice of the members of the CMIP6 ensemble is a compromise between the models' availability at the time of the analysis and the coverage of the climate sensitivity spread of the models. All CORDEX-CORE, EURO-CORDEX and CMIP5 simulations follow the RCP8.5 scenario (Riahi et al., 2011), while SSP585 (Shared Socio-Economic Pathways, Riahi, 2017) is used for the CMIP6 ensemble. Most of the analysis was conducted based on the distribution of IPCC

AR6 regions (Iturbine et al., 2020), shown in Fig. S1 (Table 2).

2.2. The fire weather index

The Fire Weather Index (FWI) is a component of the Canadian Forest Fire Danger Rating System (Van Wagner, 1987). Although originally developed and calibrated to characterize fire behavior in a jack pine (*Pinus banksiana*) stands typical of Canadian boreal forests, its computational efficiency and limited input requirements have led to widespread adoption in various countries. The index has demonstrated good performance even in ecosystems markedly different from the boreal environment, as indicated by studies such as Di Giuseppe et al. (2016) and De Rigo et al. (2017). The European Centre for Medium-Range Weather Forecasts (ECMWF) has played an important role in advancing our understanding of weather-related risks, including the increasingly pressing issue of wildfires. The Global ECMWF Fire Forecast (GEFF) System developed by ECMWF (Di Giuseppe et al., 2020) supports the assessment and prediction of fire danger conditions by integrating relevant meteorological and environmental factors. The FWI calculation solely relies on atmospheric variables, without incorporating information about the current vegetation conditions. This approach estimates the physical potential for fire ignition and spread driven by climate forcing. As such, the FWI provides a robust climatic indicator of fire danger under global warming, independent of transient changes in vegetation cover. The FWI system follows a modular structure (see Fig. 1), where each component builds upon fuel *moisture conditions to determine the potential for fire spread and intensity*. Three fuel moisture components quantitatively track drying processes at different organic layer depths: the Fine Fuel Moisture Code (FFMC) represents the rapid response of fine surface fuels to atmospheric forcing and a primary driver of ignition likelihood; the Duff Moisture Code (DMC) captures the moisture status of intermediate duff-layers, which dry more slowly than surface fuels and therefore reflect persisent changes in weather conditions; the Drought Code (DC) quantifies long-term seasonal dryness in deep, compact organic matter. These moisture codes directly influence fuel availability. Fire behavior potential is then derived through two intermediate indices: the Initial Spread Index (ISI), which combines FFMC with wind speed to represent the expected rate of fire spread under given conditions, and the Build-Up Index (BUI), which integrates DMC and DC to estimate the total amount of combustible fuel available for sustained burning. Finally, the Fire Weather Index (FWI) non-linearly combines ISI and BUI to represent the potential fire intensity. Through this hierarchical structure, the FWI links meteorological variability to fuel dryness and the capacity for fast-spreading, high-intensity fires (Van Wagner, 1987; Wotton, 2009).

For the sake of conciseness, we have just briefly reviewed the fundamental concepts behind the FWI system. For a comprehensive explanation of the FWI system, the interactions between the various components, and how these are employed in fire management, we refer to Van Wagner (1987) and Wotton (2009).

Indicators of fire danger are provided by the Fire Weather Index system based on four weather factors: temperature, relative humidity, precipitation, and wind speed (Van Wagner, 1987). The FWI requires daily 24-hr accumulated precipitation as well as temperature, humidity, and wind speed at 1 200 local time. However, due to challanges in obtaining both observed and modeled data at 12:00 local time, many studies compute the FWI on a daily basis (Carvalho et al., 2010; Giannakopoulos et al., 2009; Moriondo et al., 2006, Bento et al., 2023). To represent the worst case scenario we use daily maximum temperature, daily wind speed, daily accumulated precipitation and daily relative humidity for historical (1980–2005) and future (2006–2099) experiments. Regions where more than 80% of their existing land cover is classified as water, snow/ice, or barren/sparsely vegetated by MODIS land cover type product (Friedl et al., 2010) are considered unburnable and masked out of the analysis (see Fig. S1).

2.3. Estimating fire danger using FWI danger classes

The Fire Weather Index was calculated on a daily basis for each calendar year (1 January to 31 December) over the period 1980–2099 for all climate model ensemble members. To facilitate the interpretation of the FWI, we used six fire danger classes proposed by the European Forest Fire Information System (EFFIS; EFFIS, 2021), each class representing a different level of wildfire risk: low, medium, high, very high, extreme, very extreme (see Table 4). The FWI danger classes are essential tools for wildfire management and prevention strategies. They

Table 3
CMIP6 models used in this study.

CMIP6	Ensemble
CNRM-CM6-1	r1i1p1f2
EC-Earth3-Veg	r1i1p1f2
CanESM5	r1i1p1f2
MIROC6	r1i1p1f2
HadGEM3-GC31-LL	r1i1p1f2
MRI-ESM2-0	r1i1p1f2
NorESM2-LM	r1i1p1f2

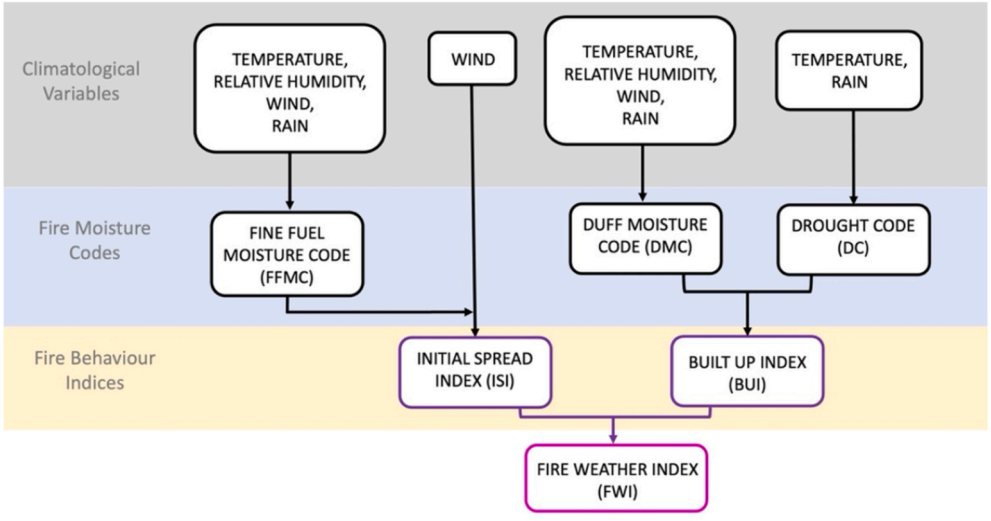

Fig. 1. Flowchart of the Canadian Forest Fire Weather Index (FWI) system used in this study (Van Wagner, 1987).

Table 4
The Fire danger classes according to EFFIS.

FWI category	FWI values
LOW	0 - 11.2
MODERATE	11.2 -21.3
HIGH	21.3 - 38
VERY HIGH	38 - 50
EXTREME	50 - 70
VERY EXTREME	>=70

Table 5
Percentage of emerged burnable land areas for each Global Warming Level and for each ensemble.

	CORDEX (% emerged)	CMIP5(% emerged)	CMIP6(% emerged)
GWL 1.0	3.44%	14.87%	9.23%
GWL 1.5	26.79%	47.29%	41.51%
GWL 2.0	46.59%	67.92%	53.00%
GWL 3.0	72.15%	71.96%	69.82%
GWL 4.0	79.75%	74.39%	81.75%

provide actionable information to guide preparedness and response measures, such as resource allocation, fire restricions, and public saftey notifications, with the goal of reducing wildfire impacts on ecosystems and society.

2.4. Time of Emergence (ToE)

The concept of "time of emergence" is crucial in various fields, ranging from climate science to technological innovation. In climate science, the ToE is used as an indicator of when the forced signal of climate change becomes distinguishable from the background noise of natural variability. Specifically, TOE marks the moment when a given climate variable, such as temperature, precipitation, or in our case fire-weather, exceeds the range of variability observed under historical conditions, making the influence of anthropogenic climate change detectable. In this study, we define TOE as the year when the increase in the Fire Weather Index (FWI) rises above the upper bound of its internal-variability envelope. The envelope is computed using ± 2 standard deviations of the climate-model ensemble distribution over a reference historical period (1980–2010). TOE is then identified as the first year in which the 30-year running mean of the ensemble-mean FWI exceeds this upper bound.

This approach is consistent with the widely used $\pm 2\sigma$ detectability criterion, approximating a 95% confidence range for internal variability (e.g., Hawkins and Sutton, 2012). By requiring the forced signal to exceed this threshold, we ensure that emergence is attributed to anthropogenic climate change rather than fluctuations expected under natural variability alone. To assess the robustness of our TOE estimates, we complement this confidence-interval method with a signal-to-noise (S/N) threshold analysis, where emergence is detected once the forced change in FWI exceeds a multiple of the simulated interannual variability. We use $S/N > 1$ as our central criterion (signal larger than noise, as previously done by Hawkins and Sutton, 2012; Hawkins et al., 2020; Dosio et al., 2025).

2.5. Global Temperature of Emergence (GToE)

Following Hawkins and Sutton (2012), we also evaluate the emergence of fire-weather signals as a function of global warming rather than time, using the Global Temperature of Emergence (GToE) framework. Unlike ToE, which depends on the evolution of emissions in time, GToE expresses the detectability of change directly as a funcion of global mean surface temperature increase relative to pre-industrial conditions. This provies a scenario-independent metric that is more closely aligned with policy targets such as for example the Paris Agreement. GToE is defined on the basis of thresholds of temperature, the Global Warming Levels, expressed as changes in surface global temperature relative to the pre-industrial period (1850–1900). In the present work, we assess emergence at five Global Warming Levels (GWLs): 1.0°, 1.5 °C, 2.0 °C, 3.0 °C, and 4.0 °C. Consistent with the S/N-based detectability approach outlined in Section 2.4, we diagnose emergence for each model when the forced FWI signal exceeds internal variability. To ensure robustness, following the IPCC AR6 WGI Atlas metodology for defining robust climate change signals (Cross-Chapter Box Atlas.1), a region is considered to have emerged when *(i)* at least 66% of models satisfy $S/N > 1$, to ensure consistent detection of signals emerging from natural variability, and *(ii)* at least 80% of them agree on the sign of change, to reduce false positives while recognizing increased multi-model agreement in future projections. The signal-to-noise ratio is estimated for each model from the ratio between the change and the standard deviation of the reference period 1980–2010. This complementary diagnostic allows us to identify not only when but under what level of global warming fire-weather conditions become detectably more sever, supporting impact-relevant interpretation of the results, highlighting the urgency of adaptation in tregions where emergence occurs already below 1.5 °C of global warming.

3. Results

3.1. Validation vs GEFF-ERA5

The FWI is not a directly observable quantity, being an index quantifying potential danger. It can be however validated against existing reanalysis products. This section examines how the FWI obtained using CORDEX-CORE, CMIP5 and CMIP6 data compares to reanalysis products, such as the data from the Global ECMWF Fire Forecast model (hereafter GEFF-ERA5; Vitolo et al., 2019). Developed by the European Forest Fire Information System under the Copernicus Emergency Management Service, GEFF-ERA5 provides daily, continuous fire weather data with a spatial resolution of 0.25° across the global land surface. GEFF-ERA5 is based on input fields from the ERA5 Reanalysis (ERA5; Hersbach et al., 2020) and covers the period from 1979 to the present.

Before investigating the climate change signal on the FWI, we are interested in assessing the model's ability in reproducing the observed trend in fire-weather conditions. Fig. 2 shows the spatial patterns of statistically significant linear trends over 1980–2005 of the three ensembles analyzed. Hatched lines cover areas where changes are not significant at the 95% confidence level (Student's *t*-test). Areas of large positive trends are seen over all the continents for the reanalysis, more intense on continental South America, Central-Eastern Africa, South Africa, Western North America and Northern Central America, West Central-Asia and East Asia; a negative trend is present over the Indian peninsula. The spatial pattern is globally well represented by the CORDEX-CORE ensemble, that is overall more consistent with GEFF-ERA5 in representing a significant positive trend but weaker over Western and Central-Eastern Africa, South Africa, Western North America and Northern Central America, West Central-Asia and East Asia and the northern part of continental South America. The negative trend over the Indian continent is weaker and not significant, while a significant positive trend is shown over la Plata basin opposite to GEFF-ERA5. The CMIP5 models show similar trends to GEFF-ERA5 only in some regions like West Central-Asia and the northern part of continental South America, but with reduced spatial extent, with significant

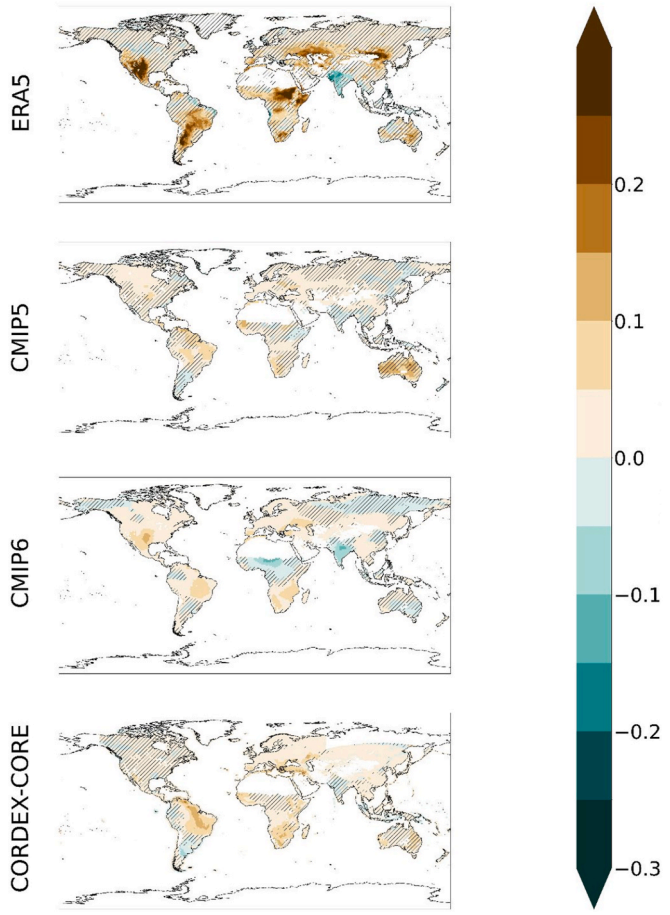

Fig. 2. Fire Weather Index trend (left) for the historical period 1980–2023. The signal is masked-out by the unburned areas given by the GFED4 dataset (Giglio et al., 2013). Dashed lines cover areas where changes are not significant at the 95% confidence level (Mann Kendall test for the ERA5, Student's *t*-test for the ensembles).

opposite to GEFF-ERA5 positive trends in South America and Australia. CMIP6 shows a negative trend over the Sahel regions, in disagreement with the reanalysis, and positive weaker trends over Southern Africa, the northern part of continental South America, Western North America and Northern Central America, West Central-Asia and East-Asia and a significant negative trend over the Indian peninsula, similarly to ERA5. We calculated the percentage of grid points where the trends have the same sign as ERA5: 81.46% for CORDEX, 74.44% for CMIP5, and 71.32% for CMIP6.These results suggest that CORDEX-CORE has a more accurate representation of observed FWI trends. The CORDEX-CORE ensemble better captures both the direction and spatial distribution of changes compared to CMIP5 and CMIP6. While CMIP5 and CMIP6 reflect some regional patterns, their overall alignment with reanalysis is weaker, especially over Africa and South America. This suggests the use of the CORDEX ensemble for regional assessments of future fire weather. It also points out the greater uncertainties linked to global model ensembles.

3.2. FWI changes

We have used the IPCC AR6 regions (Iturbine et al., 2020), to assess regional changes of the FWI index and the four meteorological variables associated with it. We excluded the SAH, ARP, and ECA regions from the analysis because the percentage of grid points available for analysis after masking was lower than 30%. In Fig. 3 heatmaps show projected multi-model mean changes for each region and ensemble (CORDEX-CORE, CMIP5 and CMIP6). Variables include: (a) maximum temperature change (ΔTmax, °C), (b) precipitation change (ΔPr, %), (c) relative humidity change (ΔHurs, %), (d) near-surface wind change (ΔSfcWind, %), and (e) change in Fire Weather Index (ΔFWI, %) for all AR6 regions, at different global warming levels (GWLs) (rows from bottom to top correspond to 1.0 °C, 1.5 °C, 2.0 °C, 3.0 °C and 4.0 °C GWLs). A detailed list of the change values for each region and variable are shown in Table TS1-TS5 in the Supplementary Material. AR6 regions are ordered in the x-axis according to latitude (from north to south). Spatial analyses indicate a widespread increase in FWI values across all the regions. Changes in Fire Weather Index (FWI) align closely with the projected changes in the four meteorological variables needed for the FWI calculation. Increases in maximum air temperature (*tasmax*), reaching up to 6 °C, and a maximum decline between 4% and 12% in relative humidity (*hurs*) are associated with the stronger increase of FWI for all the 3 model ensembles and across the majority of regions.

To understand which of the four variables play a major role in impacting the projected fire weather index we performed a correlation of the FWI changes with the changes of the four variables used to calculate the index. We analyzed the statistically significant correlations at the 95% confidence level between the values in table TS1 with the values in tables TS2-TS5, finding that the main drivers are *tasmax* (correlation 0.68) and *hurs* (correlation −0.57) and 0.19 and −0.04 for wind and precipitation respectively. If we restrict the analysis to the tropical regions, the relative humidity becomes the main driver with a higher negative correlation (−0.71), suggesting that lower humidity significantly increases fire risk, especially in tropical regions where moisture availability is a key limiting factor, followed by tasmax (0.66), by precipitation (−0.32) and by wind (0.35). The opposite is observed when considering the subsets of regions in the extra-tropics, where the correlation is higher for *tasmax* (0.74 for the Northern-Extratropics, 0.69 for the Southern Extratropics) and lower for the relative humidity *hurs* (−0.50 for the Northern-Extratropics, −0.56 for the Southern Extratropics). Precipitation correlations are lower in all the regions, in the Tropics (−0.32) and Southern Extratropics (−0.40), precipitation is negatively correlated with FWI, meaning that wetter conditions reduce fire risk, as expected. The decrease in relative humidity in the extratropics has a greater impact on fire weather conditions than the increase in wind speed in the tropics, as tropical regions generally maintain higher baseline humidity levels compared to extratropical regions. In the tropics, higher humidity can act as a limiting factor for fire spread, whereas in the extratropics, reductions in humidity can lead to significant drying of fuels, thereby increasing fire risk substantially.

At all warming levels, maximum temperatures are projected to increase, with more intense warming in northern regions like CNA, WNA, NEN, WCA,. The increase in *ΔTasmax* for tropical regions like CAR and SAS, as well as in South America (SES, SSA and SWS), is generally less extreme compared to northern regions (Fig. 3 and TS3).

The Mediterranean region (MED) shows a strong decrease in precipitation as global warming levels increase for all the ensembles. South Asia (SAS) shows an increase in precipitation for the three ensembles, reflecting the complex effects of warming on monsoon patterns and confirming the negative FWI trends highlighted in Fig. 2. With a few exceptions, the overall trend shows a decrease in humidity across most regions (Fig. 3 and TS3). South America (NES, NSA, SAM), the Mediterranean (MED), and Southern Africa (WSAF) experience the largest reductions in relative humidity (ΔHurs) as global warming intensifies. This decline may worsen arid conditions, heightening drought risks in areas that are already dry, thus increasing the fire risk too.

The strongest increases in FWI are projected for tropical areas such as NSA, NWS, SAM, SEA, driven by rising temperatures combined with reduced relative humidity and enhanced wind conditions. Substantial increases are also found in well known extra-tropical fire-prone areas such as MED (associated with reduced relative humidity, wind and precipitation), as well as WCE and WNA (associated with reduced relative humidity, wind and increases precipitation). These consistent

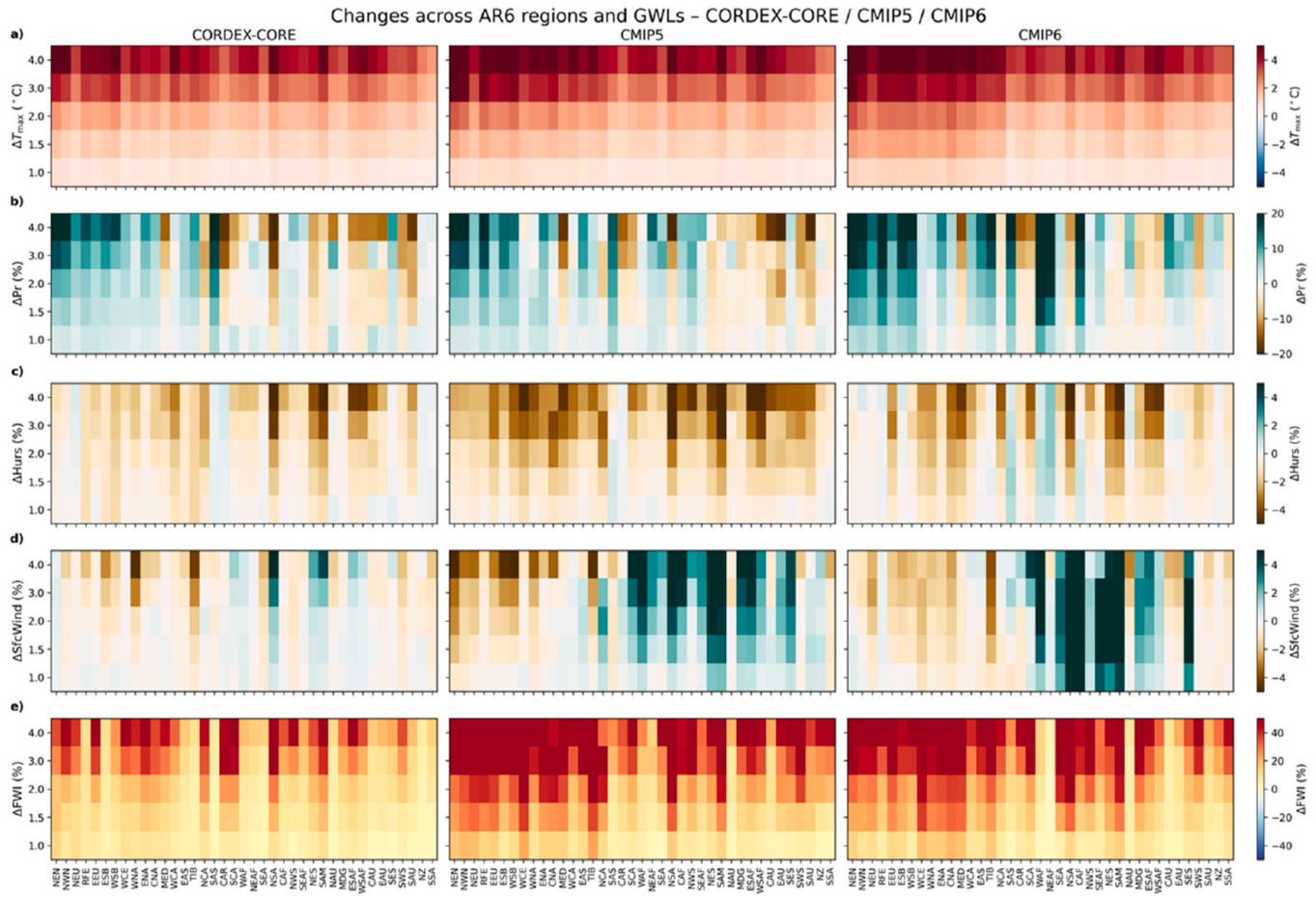

Fig. 3. Regional climate change signals across AR6 land regions under five global warming levels. Heatmaps show projected multi-model mean changes for each region and ensemble (CORDEX-CORE, CMIP5 and CMIP6). Variables include: (a) maximum temperature change (ΔTmax, °C), (b) precipitation change (ΔPr, %), (c) relative humidity change (ΔHurs, %), (d) near-surface wind change (ΔSfcWind, %), and (e) change in Fire Weather Index (ΔFWI, %).

signals across all warming levels indicate that these regions are particularly vulnerable to future fire risk, even at lower warming levels.

As FWI changes in percentage may not be representative of its actual impact, we decided to express them in danger categories. Fig. 4 shows the projected changes in the FWI danger categories across various AR6 regions at different global warming levels. For each AR6 region, the vertical bars represent the regional average FWI category for REF, GWL1.0, GWL1.5, GWL2.0, GWL3.0, and GWL4.0 (from bottom to top). A circle in the middle of each bar indicates the maximum category reached within the region. Its size scales with the highest FWI value recorded within that class, as specified in the legend. A table listing the danger categories and the maximum value of FWI for each region, is available as supplementary material (TS6). The three ensembles are quite in agreement in indicating that the regions with higher risk categories are the West Africa (WAF), Central Africa (CAF), and Southern Africa (WSAF, ESAF), the Australian continent, the Mediterranean region (MED) and the Western central Asia (WCA) where all ensembles project a substantial shift toward Extreme (50–70) or Very Extreme (>70) FWI categories at GWL3.0 and GWL4.0. In regions with historically low fire risk (e.g., Northern Europe, Northeast Asia, and Northern North America), all ensembles consistently show only moderate or zero increases in FWI. CORDEX ensemble projects higher FWI categories compared to CMIP5 and CMIP6, especially in Africa, South America, and parts of Australia.

3.3. Regional patterns of time of emergence

Fig. 5 shows the time of emergence of anthropogenic climate change for each AR6 region and for each ensemble. Different shapes and colors represent the ToE according to the three different model ensembles: triangles for CORDEX models, circles for CMIP5 and squares for CMIP6 models. The gradient of colors represents the year of emergence, spanning from 2010 to present day (respectively from black to red in the colorbar) and from 2026 to 2040 (purple gradient). Darker colors signify earlier emergence, while lighter colors point to later emergence. From Fig. 5 it is evident that the climate change signal has already emerged in most areas of the globe including Europe, portions of South America, North America and South Africa and there is a consensus among all the 3 model ensembles. This signal is consistent with the development of geographic regions experiencing heightened drought risk due to anthropogenic climate change (Greve and Seneviratne, 2015; Chiang et al., 2021). We find an earlier Time of Emergence (in the 2030s) in regions where fire is already a well-known issue, such as the Amazon forest, Central America, the Mediterranean, and South Africa. By contrast, in South-East Asia and North America the signal has not yet emerged. We assess the differences in emergence year among the three ensembles (CORDEX, CMIP5, CMIP6) across all AR6 regions. The distribution of inter-ensemble year differences (bottom box in Fig. 5) shows a strong clustering within a few years (median ≈ 6 years), with only a few outliers displaying larger gaps. This indicates a robust agreement across models: all ensembles consistently suggest that the signal has already emerged or will emerge imminently in most regions. Although regional differences can arise from factors such as model resolution, physical parameterizations, and the representation of local processes, these timing offsets remain relatively small when placed in the context of centennial-scale climate projections. Importantly, all ensembles

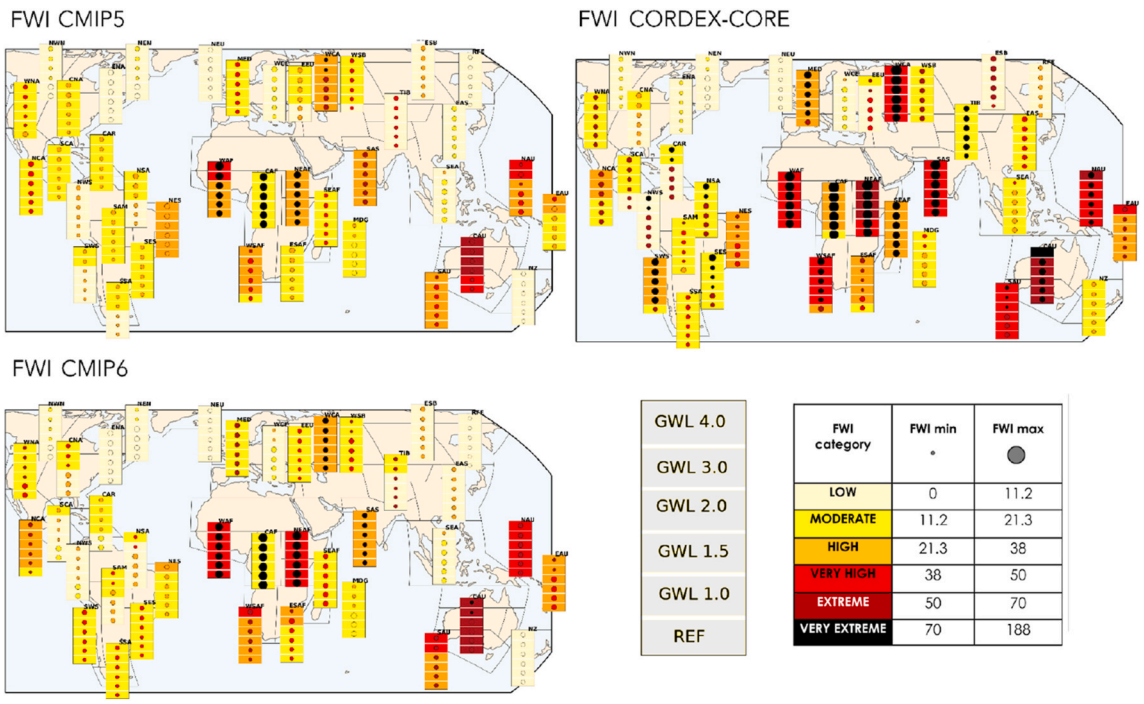

Fig. 4. FWI changes expressed in danger categories, for different global warming levels. For each AR6 region, vertical bars show the regional average FWI category for the REF, GWL1.0, GWL1.5, GWL 2.0, GWL 3.0, GWL 4.0 (from bottom to top). In the middle of each bar a circle shows the maximum FWI category in each region. The size of the circle is proportional to the maximum value of FWI in each category within the range reported in the legend.

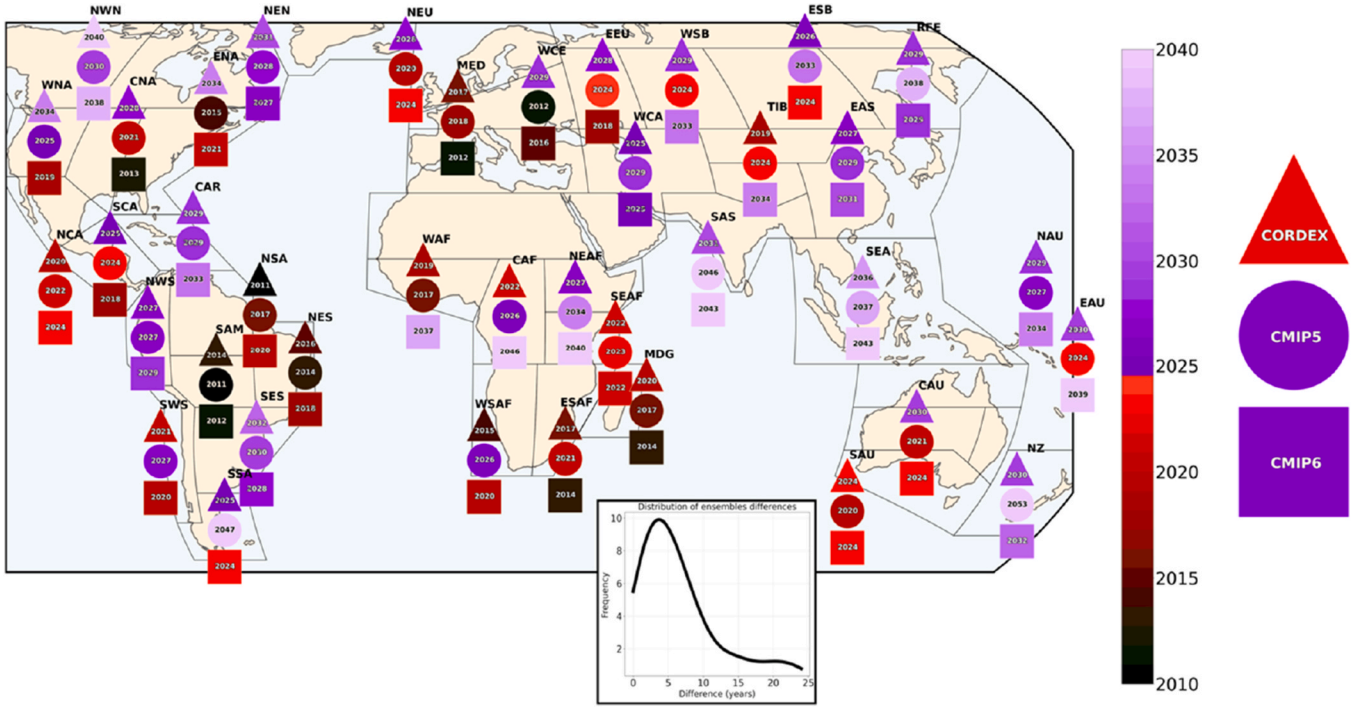

Fig. 5. Time of emergence of anthropogenic climate change for the Fire Weather Index for each AR6 region for each ensemble. The box in the bottom shows the distribution of ensemble emergence year differences.

consistently indicate that the emergence of fire-weather risk is already occurring or imminent in these regions. This reinforces the robustness of our conclusions: despite differences in model characteristics, the emergence signal is strong and persistent across modelling frameworks.

3.4. Global Temperature of Emergence (GToE)

Fig. 6 displays the probability of exceeding five Global Warming Levels (GWLs) - 1.0 °C, 1.5 °C, 2.0 °C, 3.0 °C, and 4.0 °C - for the FWI across the three climate model ensembles. Each panel shows the likelihood of crossing a specific GWL threshold, with higher probabilities

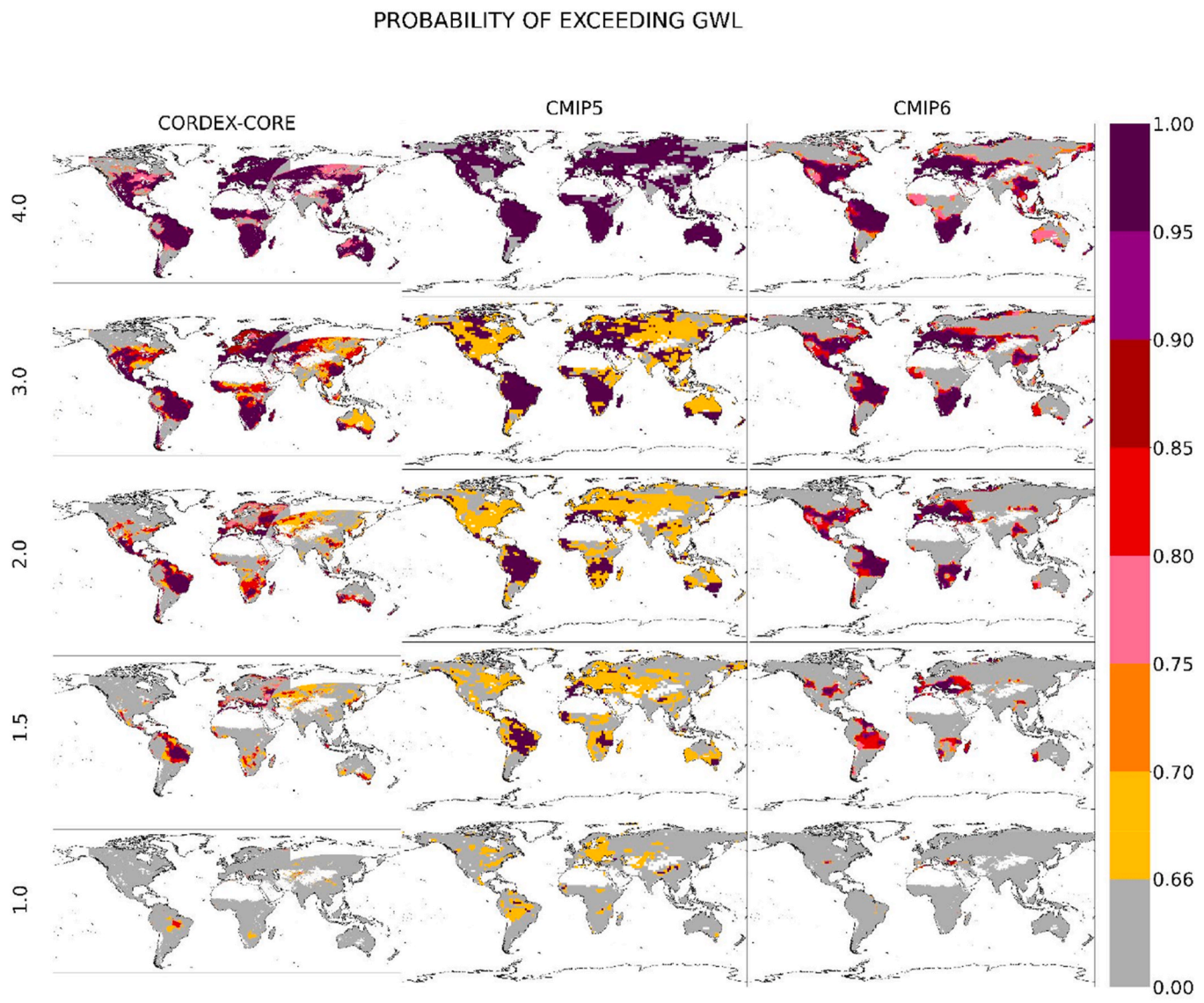

Fig. 6. Probability of exceeding the GWL 1.0, 1.5, 2.0, 3.0 and 4.0 for the FWI. The signal is masked-out by the unburned areas given by the GFED4 dataset (Giglio et al., 2013).

(darker shades) indicating a stronger likelihood of fire weather intensification at a specific warming level. All the 3 ensembles have extensive areas where signals are emerging already at 1.5 °C, with a percentage of burnable land grid-points of 26.79%, 47.29% and 41.51% for CORDEX, CMIP5 and CMIP6 ensembles respectively. The percentages are then increasing up to 79.75%, 74.39% and 81.75% for the highest GWL (Table 5).

While informative, these global-average values mask significant spatial variations. We expanded the GToE analysis to the AR6 regions in order to investigate this regional dimensions. The resulting breakdown (see Figure FS2, showing **trends in the percentage of emerged grid points for each AR6 region** across increasing global warming levels) reveals consistent geographical patterns among the ensembles, while also identifying specific regions where ensemble disagreements are more pronounced. In regions characterized by the strongest fire danger increase (e.g., Southern Africa, Europe, North America, Northern Australia), the steepest changes are consistently found in the CORDEX-CORE results. This confirms that the sharper regional signals are primarily due to the downscaling approach rather than differences between CMIP5 and CMIP6 driving GCMs. The two global model ensembles show largely comparable behaviour in most regions. Overall we can say that there is a strong consensus among all model ensembles that fire weather risk is emerging as a hazard in many regions of the world starting from GWL 1.5 °C, due to climate change. It is interesting to note which are the regions where the signal does not emerge: India, the La Plata Basin, and the Horn of Africa, which is in line with the projected increases in precipitation in those regions. The area with the greatest discrepancy between the ensembles is Australia, where for CMIP6 the signal hardly emerges anywhere for any Global Warming Level (GWL).

3.5. *Seasonal length*

The lengthening of fire seasons is a notable phenomenon observed over the past decades in different regions of the world (Silva et al., 2023; Jain et al., 2017). Warmer temperatures contribute to earlier snowmelt and to the drying of vegetation, extending the period during which conditions are favorable for wildfires (Wotton and Flannigan, 1993; Wasserman and Mueller, 2023; Riley and Loehman, 2016). This prolonged fire season amplifies the overall fire risk and challenges traditional strategies for fire management. We define the fire weather season length as days per year exceeding the midrange point (average of maximum and minimum value of FWI), for each year in each grid cell

following Jolly et al. (2015).Fig. 7 shows regional significant trends (according to the Mann_Kendall test) of the season length of the FWI. Each region has a small subplot that highlights the trend over time, with the vertical axis representing the fire season length in days per year and the horizontal axis representing the years (1980–2099). The three lines in each regional subplot correspond to the three climate ensemble datasets. Across all regions, the fire season length shows a general increase over time, although the rate of increase varies by region and dataset. CORDEX generally projects a stronger trend and a larger increase in fire season length compared to CMIP5 and CMIP6 in most African regions, in South America, in Central and Eastern Asia and in the Mediterranean region. CMIP5 shows higher trends and larger increases in Central and North America and South-East Asia and Australia, while CMIP6 tends to have the most moderate trends and increases in mostly all the regions.

4. Discussion and conclusion

Anthropogenic climate change is already changing fire weather conditions globally, and this trend will accelerate over the next few decades, according to our multi-dataset and multi-threshold assessment. *By integrating multiple global and regional climate model ensembles (CMIP5, CMIP6, and CORDEX-CORE) and applying a consistent Time of Emergence methodology based on signal-to-noise ratios, we provide the first global assessment of when fire-weather hazard becomes detectable across the AR6 reference regions*. **The Fire Weather Index (FWI), a widely used operational indicator of atmospheric fire danger, responds strongly to changes in temperature, humidity, wind and fuel drying.** The mechanisms driving the increase in FWI are found to be common to all the three ensembles and differ from the equator compared to the higher latitudes. In tropical regions, the main driver of the FWI increase is the reduction in relative humidity, whereas in extratropical regions, rising temperatures are the dominant contributing factor.

Although differing in intensity, timing, and likelihood of emergence, this study highlights a strong consensus across all available datasets indicating a widespread increase in fire weather hazard across all regions. In 39% of the AR6 regions, the signal has already emerged, and it is projected to emerge in all regions by 2040 at the latest. Furthermore 26.79% of the burnable areas already exhibit an emergence of the signal at 1.5 °C global warming, increasing to 46.59%, 72.15%, and 79.75% at 2 °C, 3 °C, and 4 °C of global warming, respectively (see Table 5).

Our analysis shows clear geographical differences in the Time of Emergence (ToE) of fire weather signals. Local emergence is already noticeable in areas like the Mediterranean, southern Africa, Amazonia, and large parts of North America's high latitudes at the beginning of the 21st century. These regions overlap with previously identified climate hotspots for increasing drought risk due to human-caused climate change (Greve and Sonia, 2015; Gudmundsson and Sonia, 2016), demonstrating the strength of the signal across various hydroclimatic indicators.

As found in earlier studies, ToE tends to happen later at the local level than at broader regional levels (Maraun et al., 2013). This pattern reflects how internal variability decreases when averages are taken over larger areas. It shows why it's crucial to analyze both scales, since local-scale emergence is most relevant for impacts on ecosystems, fire management, and communities.

Spatial differences in ToE are closely linked to changes in precipitation. Regions with decreasing precipitation, such as the Mediterranean, Amazonia, southern Africa, Southeast Asia, and Australia, are among the first to reveal fire weather signals. In contrast, areas with increasing precipitation, like parts of Eurasia, North America, Argentina, and Northern Europe, tend to show later emergence. Under the high-emission RCP8.5 scenario, our results indicate a significant rise in wildfire risk in regions with strong seasonal rainfall patterns, including

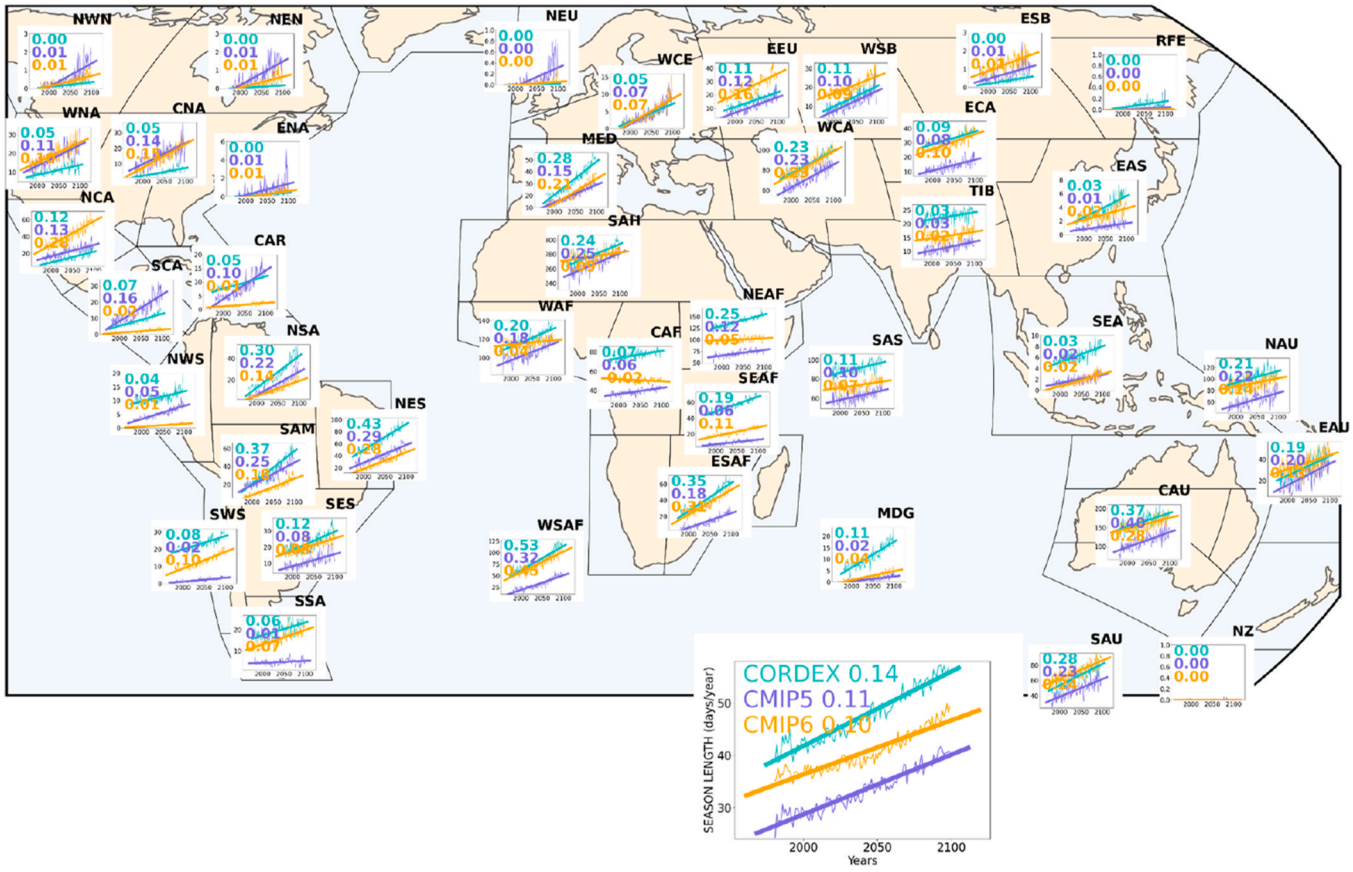

Fig. 7. Seasonal length for the AR6 regions, trends significant using Mann_Kendall test.

the Mediterranean basin and monsoonal areas in the Americas, Asia, Africa, and Oceania.

Moreover, not only does the intensity of fire weather increase, but the fire season also becomes longer. This means that in some areas, wildfires may no longer occur only in a specific season but could become a nearly year-round risk.

FWI is based on raw climate model variables (temperature, relative humidity, wind, precipitation), which typically exhibit systematic biases, especially in the humidity and wind fields. Since FWI responds nonlinearly to these inputs, such biases can propagate into the estimate and inflate or damp absolute fire-weather values (e.g., Bedia and Bhend, 2015; Vitolo et al., 2019). A comprehensive bias correction across the full multi-model ensemble is, however, not feasible in this context, especially for wind speed and relative humidity, for which high-quality, long-term observational datasets with adequate spatial coverage are limited. In addition, wind and humidity biases can only be corrected by using advanced multivariate approaches in order to preserve physical covariances, which is beyond the scope of this study. Nonetheless, our analysis primarily focuses on relative changes and emergence timing of the climate signal, metrics that are less sensitive to systematic input biases than absolute index values.

Our analysis relies on a static mask of unburnable land cover derived from conditions at present. Vegetation distribution and fuel continuity will, however, change with climate. For instance, Arctic and sub-Arctic landscapes that today are dominated by tundra and sparse vegetation will continue to experience shrub expansion and biomass accumulation, thereby reducing fuel limitations over time (e.g., Mack et al., 2011; Mack et al., 2021). Conversely, ecotonal transitions along the dryland-grassland interface can foster enhanced fire activity where fuel loads increase following episodic wet periods (Abatzoglou et al., 2021).

Accordingly, our estimates of geographic exposure to extreme fire weather, in particular within high-latitude regions and dynamic ecotones, should be considered conservative lower-bound projections that do not yet account for future vegetation changes.

Although the FWI is a widely used, reliable indicator of fire-weather conditions, it represents only potential fire danger and does not directly quantify burned area or fire occurrence. Actual wildfire impacts also depend on ignition sources such as lightning and human activities, fuel continuity and loads, vegetation management, and fire suppression. Because of this, sensitivity of fire activity to shifts in fire-weather conditions can vary substantially across regions. Several studies have shown strong empirical relationships between FWI and burned area or fire occurrence, especially in areas with abundant ignition sources and continuous fuel conditions that are receptive to burning (Abatzoglou et al., 2018; Turco et al., 2018). By contrast, areas with limited ignitions, or where management reduces fuel continuity on relatively fast timeframes, may reveal weaker or lagged responses to increased fire danger conditions (e.g., parts of Northern Europe and East Asia). Our findings therefore indicate that the projected increases in FWI, particularly across fire-prone regions such as the Mediterranean, southern Africa, Southern America and Southern Australia, are likely to be translated into increased fire risk and impacts; elsewhere, more moderate effects are likely to ensue, unless changes in ignition or fuel conditions occur in parallel. Recognition of these interactions is paramount for the interpretation of our projections and underlines the need for integrated adaptation measures that tackle not only climate-driven fire danger but also human exposure, fuel dynamics, and risk governance.

Our findings have several implications. For example, more human settlements, especially in tropical Africa, the Amazon basin, the eastern United States, and western North America, are likely to face unprecedented wildfire risks at the wildland-urban interface. This raises threats to lives, infrastructure, and economies. By knowing when and where fire weather conditions are likely to develop, gives policymakers and fire management agencies a critical opportunity to prepare. Anticipating the ToE allows for timely implementation of targeted strategies, such as strengthening prevention programs, updating land-use and building codes, and increasing investments in firefighting resources. Region-specific ToE estimates also help create better early warning systems and adapt fire danger rating systems, ensuring that preparedness keeps pace with changing fire patterns.

Our results show clear timelines that should inform adaptation planning. In regions where emergence of strong fire-weather is projected already by the 2030s, notably Southern Europe and southern Africa, investments in preparedness, such as upgrading fire-suppression capacity, hardening critical infrastructure, and developing community evacuation plans, must be prioritized over the next decade. By contrast, high-latitude parts of North America and portions of central Asia have a key opportunity to implement long-term strategies such as landscape fuel management, resilient land-use planning, and ecosystem restoration, in advance of emergence later in the century. Adaptation measures uniquely tailored to these different temporal trajectories will better mitigate future fire impacts under accelerating climate change.

CRediT authorship contribution statement

Rita Nogherotto: Writing – original draft, Visualization, Methodology, Formal analysis, Data curation, Conceptualization. **Francesca Raffaele:** Writing – review & editing, Methodology, Conceptualization. **Graziano Giuliani:** Supervision, Software, Data curation. **Erika Coppola:** Writing – review & editing, Supervision, Conceptualization.

Declaration of competing interest

The authors declare that they have no known competing financial interests or personal relationships that could have appeared to influence the work reported in this paper.

Acknowledgements

The author gratefully acknowledges Dr. Francesca Di Giuseppe for providing access to and valuable guidance in the use of the Global ECMWF Fire Forecast (GEFF) model.

We acknowledge the support from the European Union's HORIZON Research and Innovation Actions under grant agreement No 101081555, project IMPETUS4CHANGE. G.S.L.

Appendix A. Supplementary data

Supplementary data to this article can be found online at https://doi.org/10.1016/j.wace.2026.100861.

Data availability

The climate model data used in this study are publicly available from the Earth System Grid Federation (ESGF) data portal. CMIP5 and CMIP6 global model simulations can be accessed at https://esgf-node.llnl.gov.

Open-source code to run the GEFF system is available at https://github.com/ecmwf-projects/geff and precomputed GEFF runs based on ERA5 reanalyses are now available through the C3S at: https://cds.climate.copernicus.eu/cdsapp#!/dataset/cems-fire-historical?tab=overview.

References

Abatzoglou, J.T., et al., 2016. Controls on interannual variability in lightning-caused fire activity in the western US. Environmental Research Letters 11 (4), 045005.
Abatzoglou, J.T., et al., 2018. Global patterns of interannual climate–fire relationships. Glob. Change Biol. 24 (11), 5164–5175.
Abatzoglou, J.T., et al., 2021. Projected increases in western US forest fire despite growing fuel constraints. Communications Earth & Environment 2 (1), 227.
Bedia, J., Bhend, J., 2015. A Bias Correction Framework in EUPORIAS WP22: Description and Examples.

Bento, V.A., et al., 2023. The future of extreme meteorological fire danger under climate change scenarios for Iberia. Weather Clim. Extrem. 42, 100623. https://doi.org/10.1016/j.wace.2023.100623.
Bowman, D.M.J.S., et al., 2020. Vegetation fires in the anthropocene. Nat. Rev. Earth Environ. 1 (10), 500–515. https://doi.org/10.1038/s41558-020-0801-5.
Carvalho, A., et al., 2010. The impact of spatial resolution on area burned and fire occurrence projections in Portugal under climate change. Clim. Change 98, 177–197. https://doi.org/10.1007/s10584-009-9731-9.
Chiang, F., Mazdiyasni, O., AghaKouchak, A., 2021. Evidence of anthropogenic impacts on global drought frequency, duration, and intensity. Nat. Commun. 12, 2754. https://doi.org/10.1038/s41467-021-22314-w.
de Groot, W.J., Flannigan, M.D., Cantin, A.S., 2013. Climate change impacts on future boreal fire regimes. For. Ecol. Manag. 294, 35–44.
De Rigo, D., et al., 2017. Forest Fire Danger Extremes in Europe Under Climate Change: Variability and Uncertainty. Publications Office of the European Union.
Di Giuseppe, F., Pappenberger, F., Wetterhall, F., Krzeminski, B., Camia, A., Libertá, G., San Miguel, J., 2016. The potential predictability of fire danger provided by numerical weather prediction. J. Appl. Meteorol. Climatol. 55 (11), 2469–2491. https://doi.org/10.1175/JAMC-D-15-0297.1.
Di Giuseppe, F., Vitolo, C., Krzeminski, B., Barnard, C., Maciel, P., San-Miguel, J., 2020. Fire weather index: the skill provided by the European centre for medium-range weather forecasts ensemble prediction system. Nat. Hazards Earth Syst. Sci. 20, 2365–2378. https://doi.org/10.5194/nhess-20-2365-2020.
Dosio, A., Migliavacca, M., Maraun, D., 2025. How fast is climate changing? One generation is sufficient for unfamiliar heatwave characteristics to emerge in Europe. Clim. Change 178 (2), 26.
Fargeon, H., et al., 2020. Projections of fire danger under climate change over France: where do the greatest uncertainties lie? Clim. Change 160 (3), 479–493. https://doi.org/10.1007/s10584-020-02853-9.
Field, R.D., 2020. Evaluation of Global Fire Weather Database reanalysis and short-term forecast products. Nat. Hazards Earth Syst. Sci. 20 (4), 1123–1147.
Flannigan, M., et al., 2013. Global wildland fire season severity in the 21st century. For. Ecol. Manag. 294, 54–61.
Flannigan, M.D., et al., 2016. Fuel moisture sensitivity to temperature and precipitation: climate change implications. Clim. Change 134 (1), 59–71.
Friedl, M.A., Sulla-Menashe, D., Tan, B., Schneider, A., Ramankutty, N., Sibley, A., Huang, X., 2010. MODIS collection 5 global land cover: algorithm refinements and characterization of new datasets. Remote Sens. Environ. 114 (1), 168–182. https://doi.org/10.1016/j.rse.2009.08.016.
Giannakopoulos, C., le Sager, P., Bindi, M., Moriondo, M., Kostopoulou, E., Goodess, C. M., 2009. Climatic changes and associated impacts in the mediterranean resulting from a 2°C global warming. Global Planet. Change 68, 209–224. https://doi.org/10.1016/j.gloplacha.2009.06.001.
Giglio, L., Randerson, J.T., Werf, G.R., 2013. Analysis of daily, monthly, and annual burned area using the fourth-generation global fire emissions database (GFED4). J. Geophys. Res.: Biogeosciences 118, 317–328. https://doi.org/10.1002/jgrg.20042.
Greve, Peter, Sonia, I. Seneviratne, 2015. Assessment of future changes in water availability and aridity. Geophys. Res. Lett. 42 (13), 5493–5499.
Gudmundsson, L., Sonia, I.S., 2016. Anthropogenic climate change affects meteorological drought risk in Europe. Environ. Res. Lett. 11 (4), 044005.
Hawkins, E., Frame, D., Harrington, L., Joshi, M., King, A., Rojas, M., Sutton, R., 2020. Observed emergence of the climate change signal: from the familiar to the unknown. Geophys. Res. Lett. 47 (6) e2019GL086259.
Hawkins, E., Sutton, R., 2012. Time of emergence of climate signals. Geophys. Res. Lett. 39, L01702. https://doi.org/10.1029/2011GL050087.
Hersbach, H., et al., 2020. The ERA5 global reanalysis. Q. J. R. Meteorol. Soc. 146 (730), 1999–2049.
Iturbine, M., et al., 2020. An update of IPCC climate reference regions for subcontinental analysis of climate model data: definition and aggregated datasets. Earth Syst. Sci. Data 12 (4), 2959–2970. https://doi.org/10.5194/essd-12-2959-2020.
Jain, P., Wang, X., Flannigan, M.D., 2017. Trend analysis of fire season length and extreme fire weather in North America between 1979 and 2015. Int. J. Wildland Fire 26, 1009–1020. https://doi.org/10.1071/WF17008.
Jolly, W., Cochrane, M., Freeborn, P., et al., 2015. Climate-induced variations in global wildfire danger from 1979 to 2013. Nat. Commun. 6, 7537. https://doi.org/10.1038/ncomms8537.
Kasischke, E.S., Turetsky, M.R., 2006. Recent changes in the fire regime across the North American boreal region—Spatial and temporal patterns of burning across Canada and Alaska. Geophys. Res. Lett. 33 (9). https://doi.org/10.1029/2006GL025677.
Kunkel, K.E., 2001. Surface energy budget and fuel moisture. In: Forest Fires. Academic Press, pp. 303–350.
Larry S., Bradshaw, Deeming, John E., Burgan, Robert E., 1984. The 1978 national fire-danger rating system: technical documentation. General Technical Report INT-169. Ogden, UT: US Department of Agriculture, Forest Service, Intermountain Forest and Range Experiment Station, 169, p. 44.
Mack, M.C., Bret-Harte, M.S., Hollingsworth, T.N., Jandt, R.R., Schuur, E.A., Shaver, G. R., Verbyla, D.L., 2011. Carbon loss from an unprecedented Arctic tundra wildfire. Nature 475 (7357), 489–492.
Mack, M.C., Walker, X.J., Johnstone, J.F., Alexander, H.D., Melvin, A.M., Jean, M., Miller, S.N., 2021. Carbon loss from boreal forest wildfires offset by increased dominance of deciduous trees. Science 372 (6539), 280–283.
Masson-Delmotte, V., P. Zhai, A. Pirani, S.L. Connors, C. Péan, S. Berger, N. Caud, Y. Chen, L. Goldfarb, M.I. Gomis, M. Huang, K. Leitzell, E. Lonnoy, J.B.R. Matthews, T. K. Maycock, T. Waterfield, O. Yelekçi, R. Yu, and B. Zhou (eds.). IPCC, 2021: Climate Change 2021: the Physical Science Basis. Contribution of Working Group I to the Sixth Assessment Report of the Intergovernmental Panel on Climate Change. Cambridge University Press, Cambridge, United Kingdom and New York, NY, USA, 2391 pp. doi:10.1017/9781009157896.
Maraun, Douglas., 2013. When will trends in European mean and heavy daily precipitation emerge? Environ. Res. Lett. 8 (1), 014004.
McArthur, Alan Grant, 1967. Fire behaviour in Eucalypt forests, 35.
Moriondo, M., Good, P., Durao, R., Bindi, M., Giannakopoulos, C., Corte-Real, J., 2006. Potential impact of climate change on fire risk in the mediterranean area. Clim. Res. 31, 85–95. https://doi.org/10.3354/cr031085.
Pereira, M.G., et al., 2005. Synoptic patterns associated with large summer forest fires in Portugal. Agric. For. Meteorol. 129 (1–2), 11–25. https://doi.org/10.1016/j.agrformet.2004.11.004.
Pyne, S.J., 1996. Wild hearth: a prolegomenon to the cultural fire history of northern Eurasia. In: Fire in Ecosystems of Boreal Eurasia. Springer, Netherlands, pp. 21–44.
Riahi, K., van Vuuren, D.P., Klimont, Z., Smith, S.J., Leggett, J., 2011. Representative concentration pathways: an overview. Clim. Change 109 (1–2), 5–31. https://doi.org/10.1007/s10584-011-0148-z.
Riahi, K., 2017. The shared socioeconomic pathways and their energy, land use, and greenhouse gas emissions implications: an overview. Glob. Environ. Change 42, 153–168. https://doi.org/10.1016/j.gloenvcha.2016.12.008.
Riley, K.L., Loehman, R.A., 2016. Mid-21st-century climate changes increase predicted fire occurrence and fire season length, Northern Rocky Mountains, United States. Ecosphere 7 (11), e01543. https://doi.org/10.1002/ecs2.1543.
Ruffault, J., et al., 2020. Increased likelihood of heat-induced large wildfires in the Mediterranean Basin. Sci. Rep. 10 (1), 13790. https://doi.org/10.1038/s41598-020-70851-3.
Silva, P., Carmo, M., Rio, J., Novo, I., 2023. Changes in the seasonality of fire activity and fire weather in Portugal: is the wildfire season really longer? Meteorology 2 (1), 74–86. https://doi.org/10.3390/meteorology2010006.
Skinner, W.R., et al., 1999. The association between circulation anomalies in the mid-troposphere and area burned by wildland fire in Canada. Theor. Appl. Climatol. 63, 89–105. https://doi.org/10.1007/s007040050073.
Touma, D., et al., 2021. Human-driven greenhouse gas and aerosol emissions cause distinct regional impacts on extreme fire weather. Nat. Commun. 12 (1), 212. https://doi.org/10.1038/s41467-020-20673-4.
Turco, M., Rosa-Cánovas, J.J., Bedia, J., Jerez, S., Montávez, J.P., Llasat, M.C., Provenzale, A., 2018. Exacerbated fires in mediterranean Europe due to anthropogenic warming projected with non-stationary climate-fire models. Nat. Commun. 9 (1), 3821.
Van Wagner, C.E., 1987. Development and Structure of the Canadian Forest Fire Weather Index System. Canadian Forestry Service, Headquarters, Ottawa, 35.
Viegas, D.X., Viegas, M.T., 1994. A relationship between rainfall and burned area for Portugal. Int. J. Wildland Fire 4 (1), 11–16. https://doi.org/10.1071/WF9940011.
Viegas, D.X., et al., 2001. Estimating live fine fuels moisture content using meteorologically-based indices. Int. J. Wildland Fire 10 (2), 223–240. https://doi.org/10.1071/WF01023.
Vitolo, C., Di Giuseppe, F., Krzeminski, B., San-Miguel-Ayanz, J., 2019. Data descriptor: a 1980–2018 global fire danger re-analysis dataset for the Canadian fire weather indices. Sci. Data 6, 32. https://doi.org/10.1038/sdata.2019.32.
Wasserman, T.N., Mueller, S.E., 2023. Climate influences on future fire severity: a synthesis of climate-fire interactions and impacts on fire regimes, high-severity fire, and forests in the western United States. Fire Ecol. 19 (1), 43. https://doi.org/10.1186/s42408-023-00200-8.
Westerling, A.L., 2016. Increasing western US forest wildfire activity: sensitivity to changes in the timing of spring. Phil. Trans. Biol. Sci. 371 (1696), 20150178. https://doi.org/10.1098/rstb.2015.0178.
Wotton, B.M., Flannigan, M.D., 1993. Length of the fire season in a changing climate. For. Chron. 69 (2), 187–192. https://doi.org/10.5558/tfc69187-2.
Williams, A.P., Abatzoglou, J.T., 2016. Recent advances and remaining uncertainties in resolving past and future climate effects on global fire activity. Curr. Clim. Change Rep. 2 (1), 1–14.
Wotton, B. Mike, 2009. Interpreting and using outputs from the Canadian forest fire danger rating system in research applications. Environ. Ecol. Stat. 16 (2), 107–131.